JOURNAL OF MATERIALS SCIENCE 27 (1992) 1553–1559

Prediction of a thermal shock damage map for glass plates

CHIN-CHEN CHIU, E. D. CASE
Department of Metallurgy, Mechanics and Materials Science, Michigan State University, East Lansing, MI 48824, USA

A thermal shock damage map to qualitatively predict the effect of thermal quench on a glass plate is proposed based on thermoelastic and thermoviscoelastic stress theory. The map indicates that quenching a glass plate may induce either thermal shock damage and/or residual stresses. The theoretical analysis also generally agrees with experimental results reported for the thermal quench of polycrystalline alumina specimens with a significant glassy phase.

1. Introduction

Typical thermal shock of ceramics involves quenching of hot specimens into a water bath [1–3], by which tremendous heat flow occurs and severe thermal stresses develop in the quenched component. A thermal quench may either weaken [1–6] or strengthen ceramics [7–12]. For instance, tempered glass is strengthened by thermal quenching from above the annealing temperature [7]. For polycrystalline ceramics, Travitzky *et al.* [8], Gebauer and co-workers [9, 10], and Ohira and Bradt [11] observed that for quenching aluminosilicate specimens from about 1400 °C to room temperature, silicone oil increased the retained fracture strength. Kirchner [12] observed that quenching alumina components from above 1600 °C into a silicone oil bath more than doubled the average flexural strength of the components, compared to the as-received strength. Kirchner proposed that this dramatic strength increase resulted from residual stresses induced by the quench from high temperature.

Transient thermal stresses are the driving force for thermal shock damage. Traditional studies of thermal shock damage in ceramics calculate transient thermal stresses through thermoelastic theory [1–6], which assumes that the quenched ceramics are linear-elastic materials. The assumption of linear elasticity is reasonable for brittle ceramics quenched from below the annealing temperature. However, viscous flow occurs when some ceramics are heated to near their annealing temperature (for example, soda–lime–silica glass or a glassy grain boundary phase in a polycrystalline ceramic), and hence when viscous flow occurs, the materials behave as viscoelastic materials rather than purely elastic materials. Thus for thermal quenching from above the annealing temperature, thermal stress calculations must include both thermoelastic theory and viscous flow effects.

This paper analyses the thermal shock of glass plates quenched from both above and below the glass annealing temperature. When the initial temperature of the glass plate is below the annealing temperature, the thermal stresses are calculated using thermoelastic theory [13]. When the initial temperature is above the annealing temperature, viscous flow is included and the stresses are calculated from thermoviscoelastic theory [14, 15]. Crack growth is assumed to occur if the magnitude of the transient tensile stress at the surface or the residual stress in the interior exceed the fracture strength.

2. Thermal stresses

2.1. Quench from below the annealing temperature

Non-uniform temperature distributions in an elastic heated body result in thermoelastic stresses. For this study's calculations of thermoelastic stresses in a glass plate quenched from below its annealing temperature, we assume that the material properties and thermal transfer conditions (elastic modulus, thermal expansion, thermal conductivity, thermal diffusivity, and surface heat transfer coefficient) are independent of temperature. In addition, the initial glass plate temperature and quenching medium temperature are assumed to be constant.

Heat flow out of the plate occurs as a result of the thermal quench. Heat conduction takes place in the plate and heat convection occurs in the quenching medium. The thickness of the plate is assumed to be small compared with its width and length. Thus, edge effects are neglected and the heat flow is one-dimensional. The governing equation for the heat transfer is

$$\frac{1}{a}\left(\frac{\partial T}{\partial t}\right) = \frac{\partial^2 T(Z, t)}{\partial Z^2} \quad (1)$$

where a is the thermal diffusivity, Z is the coordinate in the direction normal to glass plate surfaces, t is the time and $T(Z, t)$ is the temperature distribution in the

glass plate. The boundary and initial conditions are

$$\frac{\partial T}{\partial Z} = 0 \quad Z = 0 \tag{2a}$$

$$-K\frac{\partial T}{\partial Z} = h(T - T_0) \quad Z = l \text{ and } -l \tag{2b}$$

$$T = T_i \quad t = 0 \tag{2c}$$

where T_0 is the quenching medium temperature, T_i is the initial temperature of glass plate, h is the surface heat transfer coefficient, K is the thermal conductivity and l is the half-thickness of glass plate; $Z = l$ and $Z = -l$ on the plate surfaces.

Separation of variables gives the temperature gradient through the thickness of the plate (Z axis) as [16]

$$\Delta T_*(Z, t) = \Delta T \sum_{n=1}^{\infty} 2\left(\frac{\sin\delta_n \cos(\delta_n Z/l)}{\delta_n + \sin\delta_n \cos\delta_n}\right) \times \exp\left[-a\left(\frac{\delta_n}{l}\right)^2 t\right] \tag{3a}$$

$$\delta_n \tan\delta_n = B \quad n = 1, 2, 3, \ldots \tag{3b}$$

$$T(Z, t) = T_0 + \Delta T_*(Z, t) \tag{3c}$$

where ΔT is the quenching temperature difference between T_i and T_0, δ_n is the root of Equation 3b and B is Biot's modulus [17], which is in turn given by

$$B = \frac{rh}{K} \tag{4}$$

where r is a characteristic dimension of the specimen. For the plate geometry considered here, r is equal to the plate's half-thickness, l [17]. Without considering surface traction, the thermoelastic stresses in an infinite plate are [13]

$$\sigma_{xx}(Z, t) = \sigma_{yy}(Z, t) = \frac{\alpha E}{1 - \nu}\left(-\Delta T_* + \frac{1}{2l}\int_{-l}^{l} \Delta T_* \, dZ + \frac{3Z}{2l^3}\int_{-l}^{l} \Delta T_* Z \, dZ\right) \tag{5a}$$

$$\sigma_{zz} = \sigma_{xy} = \sigma_{xz} = \sigma_{yz} = 0 \tag{5b}$$

where E is the elastic modulus, ν is Poisson's ratio, α is the thermal expansion, σ_{zz} is the normal stress in the direction normal to the plate surface, σ_{xx} and σ_{yy} are the normal stress in the direction parallel to the plate surface, and σ_{xy}, σ_{xz} and σ_{yz} are the shear stress.

Combining Equations 3 and 5 gives

$$\sigma_{xx}(Z, t) = \sigma_{yy}(Z, t) = 2\frac{\alpha E \Delta T}{1 - \nu}\left\{\sum_{n=1}^{\infty} \exp\left[-a\left(\frac{\delta_n}{l}\right)^2 t\right] \times \frac{\sin\delta_n}{\delta_n + \cos\delta_n \sin\delta_n} \times \left[\frac{\sin\delta_n}{\delta_n} - \cos\left(\frac{\delta_n Z}{l}\right)\right]\right\} \tag{6}$$

Equation 6 thus describes the thermoelastic stresses in an infinite glass plate of thickness $2l$ quenched from below the annealing temperature.

2.2. Quench from above the annealing temperature

When a glass plate is heated to near its annealing temperature, the viscosity of the glass decreases. At the annealing temperature, viscous flow is significant. For example, internal stress in glass is substantially relieved by viscous flow during a one-hour heat treatment at the annealing temperature [18]. If a glass plate is quenched from above its annealing temperature, the transient thermal stresses are also influenced by viscous flow [14].

The mathematics of the thermal stresses in linear viscoelastic materials have been treated by several authors who account for the effect of viscous flow and stress relaxation [14, 19–24]. Lee *et al.* [14] unified the mathematical framework and presented a thermoviscoelastic theory for the thermal stresses and residual stresses that arise when a glass plate is quenched symmetrically from both surfaces. Upon comparison with experimental results, Narayanaswamy and Gardon [15] modified the numerical calculation technique of Lee *et al.* to bring the theoretical results into closer agreement with experimental data. Since the theory of Lee *et al.* can conveniently model the transient thermal stresses in a rapidly quenched glass plate, we use the formulations presented by Lee *et al.* [14] and Narayanaswamy and Gardon [15] in the present study.

Linear-elastic materials have a constant elastic modulus so that materials subjected to a given strain do not experience stress relaxation. However, linear viscoelastic materials exhibit stress relaxation for an isothermal deformation, which is described by [19, 25]

$$\sigma_{ij}(t) = \int_0^t G_{ijkl}(t - t')\frac{\partial \varepsilon_{kl}(t')}{\partial t'} dt' \tag{7}$$

where σ_{ij}, ε_{kl}, $G_{ijkl}(t)$ and t are the stress tensor, strain tensor, relaxation modulus tensor and time, respectively. For viscoelastic plates subjected to a thermal quench, Lee *et al.* [14] proposed that the transient thermal stresses may be calculated from

$$\int_0^l \sigma_{xx}(Z, t) dZ = 0 \tag{8}$$

$$\sigma_{xx}(Z, t) = 3\int_0^t R[\xi(Z, t) - \xi(Z, t')] \times \frac{\partial}{\partial t'}[\varepsilon(t') - \alpha T(Z, t')] dt' \tag{9}$$

where the reduced time, ξ, expresses the temperature and time dependence of the viscoelastic material properties. The parameter ξ is defined by [14, 20, 23]

$$\xi(Z, t) = \int_0^t \Phi[T(Z, t')] dt' \tag{10}$$

$T(Z, t)$ is the temperature distribution in the quenched glass plate (Equation 3). Lee *et al.* [14] indicated that the time-shift factor $\Phi(T)$ for soda–lime–silica glass measured at a base temperature of 538 °C is

$$\log_{10}[\Phi(T)] = 0.03861(T - 538) \tag{11}$$

$R(\xi)$ is an auxiliary modulus function associated with

the relaxation modulus tensor, G, such that for a Maxwell solid $R(\xi)$ is given by [20, 21]

$$R(\xi) = \frac{H(\xi)E_0}{3(1-\nu)}\exp\left(-\frac{\beta\xi}{\tau_0}\right) \quad (12a)$$

or

$$\bar{R}(\xi) = H(\xi)\exp\left(-\frac{\beta\xi}{\tau_0}\right) \quad (12b)$$

where

$$\beta = \frac{1+\nu}{3(1-\nu)} \quad (12c)$$

and $H(\xi)$ is the Heaviside unit step-function. E_0 and τ_0 are the instantaneous elastic modulus at $t = 0$ and the relaxation time, respectively. Batteh [26] approximated $\bar{R}$ directly from the data of Narayanaswamy and Gardon [15] for soda–lime–silica glass as

$$\bar{R}(\xi) = \exp(-\xi/700) \quad (13)$$

According to Narayanaswamy and Gardon's modification [15], Equation 9 is rewritten as

$$\sigma_{xx}(Z, t) = \sigma_{yy}(Z, t) = \frac{E_0}{1-\nu}\sum_{i=1}^{n}\left(\frac{\varepsilon(t_i) - \varepsilon(t_{i-1}) - \alpha[T(Z, t_i) - T(Z, t_{i-1})]}{\xi(Z, t_i) - \xi(Z, t_{i-1})}\int_{\xi_{i-1}}^{\xi_i}\bar{R}(\xi - \xi')\,d\xi'\right) \quad (14)$$

Equations 8 and 14 constitute a set of non-linear integral equations. To calculate the transient thermal stresses, we first numerically solve for $\xi(Z, t)$ by combining Equations 3, 10, and 11. The integral of $\int R\,d\xi'$ in Equation 14 is then calculated using Equation 13. Finally, the transient stress $\sigma(Z, t)$ and strain $\varepsilon(t)$ are calculated iteratively as a function of time t, using Equations 8 and 14. The residual stresses are the steady-state values to which $\sigma(Z, t)$ converges if time becomes great enough, for example $t = 50$ s. The residual surface stresses correspond to the convergent values, $\sigma(l, t)$. Table I lists the required input values for the numerical analysis.

3. Numerical results and discussion

For a glass plate quenched from below its annealing temperature, numerical modelling of the thermoelastic stresses shows that compressive stress arises internally in the plate and that tensile stresses develop on the plate's surface (Fig. 1a). The maximum tensile stress always appears on the surface of the glass plate.

If a glass plate is quenched from above the annealing temperature, thermoviscoelastic stresses can induce viscous flow in the glass plate which in turn leads to complex stress fields and induces residual stresses in the plate (Fig. 1b and Fig. 2). The thermoelastic surface stresses versus time increase as ΔT increases (Fig. 3a). The time evolution of the surface stresses that develop during quenching are keenly dependent on whether the plate is quenched from below or from above the annealing temperature. For quenching from below the annealing temperature, the thermoelastic stresses versus time increase monotonically as ΔT increases (Fig. 3a). In contrast, for quenching from above the annealing temperature, the thermoviscoelastic stresses generally decrease as the temperature increases (Fig. 3b).

Fig. 4 illustrates the relationship between ΔT and the maximum surface tensile stresses. For $\Delta T < 500\,^{\circ}C$, the glass plate acts as an elastic material and the stresses follow the solid line. According to Equation 6, the maximum surface tensile stresses increase linearly with increasing ΔT. For $\Delta T > 580\,^{\circ}C$,

TABLE I Numerical values used in calculating the transient thermal stresses in microscope slide glass specimens (all values measured by the present authors [27] unless otherwise indicated)

Thermal expansion, α	$8 \times 10^{-6}\,^{\circ}C^{-1}$	[5, 6]
Elastic modulus, E	70 GPa	
Poisson's ratio, ν	0.25	[5, 6]
Half-thickness of specimen, l	0.001 m	
Thermal diffusivity, a	$4.8 \times 10^{-7}\,m^2\,s^{-1}$	[5, 6]
Biot's modulus, B	10	
Quenching medium temperature, T_0	20 °C	
Flexural fracture strength	101.4 MPa	

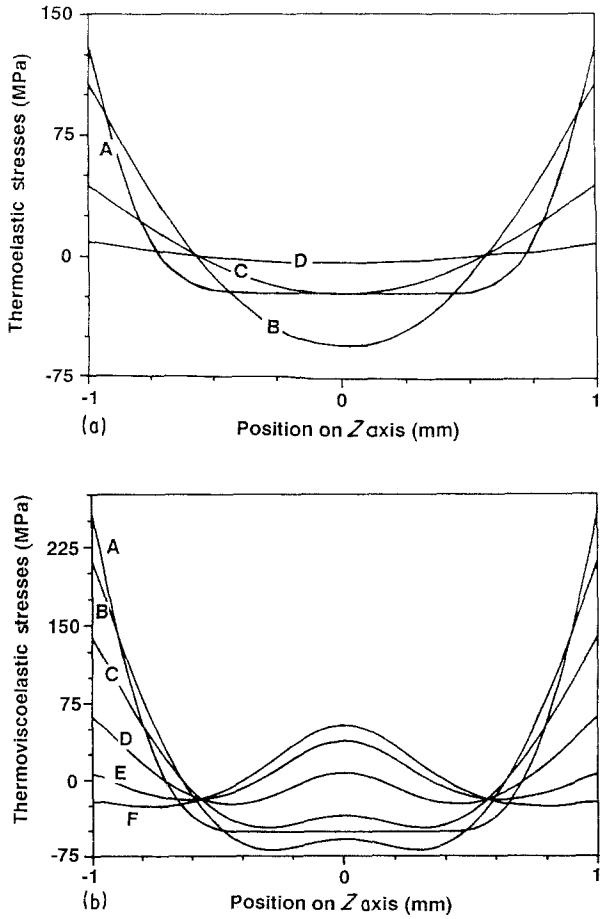

Figure 1 Transient thermal stresses in a quenched glass plate. (a) Thermal quenching from below the annealing temperature, $\Delta T = 300\,^{\circ}C$; time = (A) 0.005, (B) 0.38, (C) 1.3, (D) 2.92 s. (b) Thermal quenching from above the annealing temperature, $\Delta T = 620\,^{\circ}C$; time = (A) 0.08, (B) 0.27, (C) 0.64, (D) 1.25, (E) 2.16, (F) 3.43 s. Biot's modulus = 10.

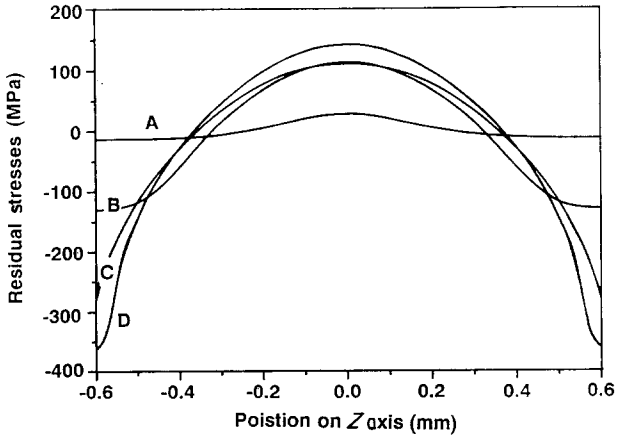

Figure 2 Residual stress profile in a glass plate quenched from above the annealing temperature. (A) $\Delta T = 620\,^{\circ}C$, Biot's modulus = 8; (B) $\Delta T = 660\,^{\circ}C$, Biot's modulus = 8; (C) $\Delta T = 700\,^{\circ}C$, Biot's modulus = 5; (D) $\Delta T = 700\,^{\circ}C$, Biot's modulus = 15.

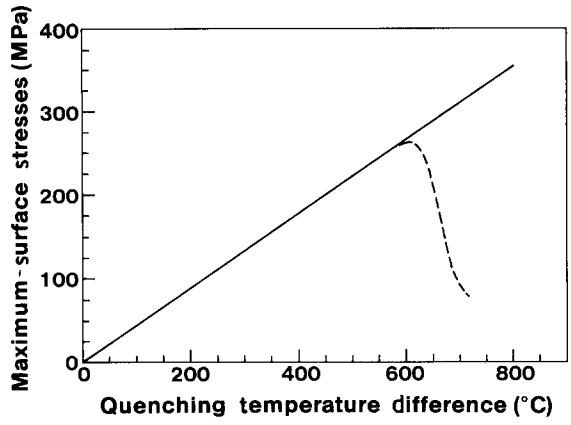

Figure 4 The maximum surface stresses in a quenched plate, as a function of the quench temperature difference ΔT: (——) thermoelastic stresses, (– – –) thermoviscoelastic stresses.

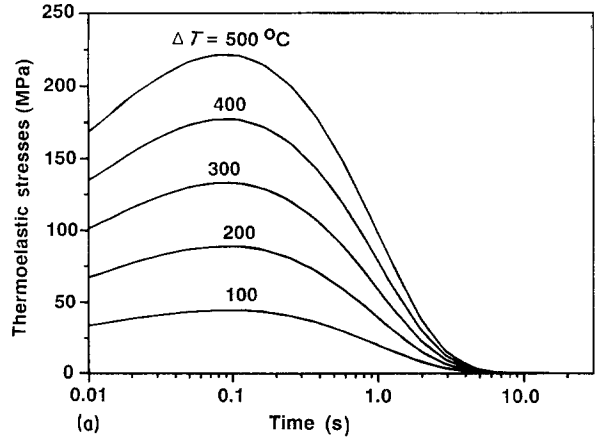

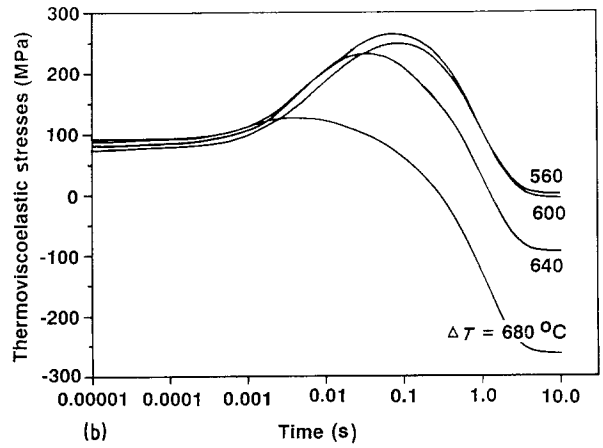

Figure 3 Influence of ΔT on surface stresses; (a) thermoelastic stresses, (b) thermoviscoelastic stresses. Biot's modulus = 10.

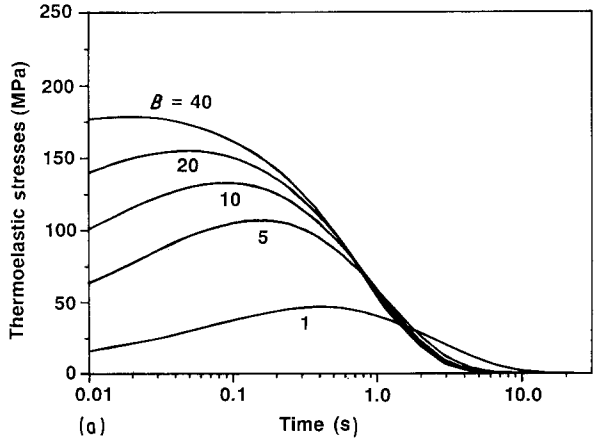

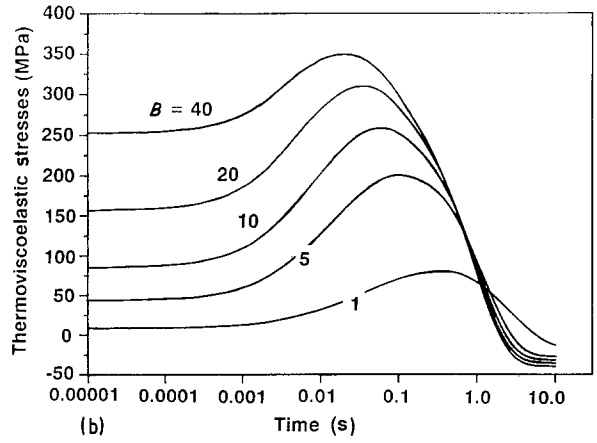

Figure 5 Influence of Biot's modulus B on surface stresses: (a) thermoelastic stresses, with $\Delta T = 300\,^{\circ}C$; (b) thermoviscoelastic stresses, with $\Delta T = 620\,^{\circ}C$.

viscous flow of the glass becomes significant, resulting in a decrease of the maximum surface tensile stresses as a function of increasing ΔT (the dashed line in Fig. 4). Between $\Delta T = 500\,^{\circ}C$ and $\Delta T = 580\,^{\circ}C$, the two curves superimpose.

The thermal stresses illustrated in Figs 1, 3 and 4 are computed for a Biot's modulus equal to 10. However, Biot's modulus influences the magnitude of thermal stresses such that as Biot's modulus increases, the maximum value of the residual tensile stress increases in the plate's interior and the transient tensile stress on the plate's surface also increases (Fig. 2 and Fig. 5a and b). Thermal quench conditions for a given material system can be described in terms of the surface heat transfer coefficient, quench temperature difference, and the specimen dimensions. However, Biot's modulus can replace both the surface heat transfer coefficient and specimen size variables such that thermal

quench conditions can be simply expressed by two variables, Biot's modulus and the quench temperature difference.

Thermal shock damage usually initiates at the regions of maximum transient tensile stress [1–6] which occurs on the surface of quenched brittle components. Crack growth also may occur in the interior of tempered glass which develops sufficiently high residual stresses. To predict the thermal shock damage of glass plates quenched from above their annealing temperature, we assume that (i) during thermal quench, crack growth is dominated by the propagation of pre-existing surface cracks; (ii) the surface layers in the initial cooling step approach elastic behaviour; (iii) the fracture strength is independent of temperature; and (iv) after the thermal quench occurs, the residual tensile stress in the interior of the quenched glass plate may be large enough to propagate pre-existing flaws. Therefore, an appropriate shock damage criterion is that the crack growth occurs if the magnitude of the transient surface stress or the residual interior tensile stress exceeds the fracture strength.

From the thermal stress calculations, we can construct a thermal shock damage map (Fig. 6) consisting of three lines, curve A for the thermoelastic stresses and curves B and C for the thermoviscoelastic stresses. The thermal quench conditions in the map are characterized by Biot's modulus and the quench temperature difference. When the thermal quench conditions correspond to a point above curves A and B, the maximum surface tensile stresses exceed the fracture strength and cracks propagate. If the quench conditions correspond to a point above curve C, crack growth is driven by the residual interior tensile stress. When the quench conditions correspond to a point below the curves, there is no shock damage. The effect of viscous flow upon the stresses becomes obvious near the annealing temperature, which is about 580 °C in this case (see Figs 4 and 6). Thus, residual thermal stresses develop in glass plates quenched from above about 600 °C.

For a thermal quench of a glass plate, three values of the critical quench temperature difference, ΔT_c, may appear on the thermal shock damage map. The critical values of ΔT_c may be calculated from the intersections of the three curves in the thermal shock damage map (Fig. 6). For example, if the glass plate is quenched at $B = 5$, the critical quench temperature differences are $\Delta T_c = 300$, 670 and 780 °C. From the three critical values, we can qualitatively infer the shape of the thermal quench strength degradation curve (Fig. 7). Glass plates quenched from below $\Delta T = 300$ °C have no thermal shock damage and their fracture strength does not change. Above $\Delta T = 780$ °C as well as between $\Delta T = 300$ °C and $\Delta T = 670$ °C, thermal shock damage reduces the retained fracture strength of the glass plate. Shock damage disappears for 670 °C < ΔT < 780 °C. The gradual increase and eventual saturation in retained fracture strength for 580 °C < ΔT < 780 °C results from viscous flow of the glass. The viscous flow decreases the magnitude of thermal stresses, which in turn decreases the probability and the severity of the thermal shock damage.

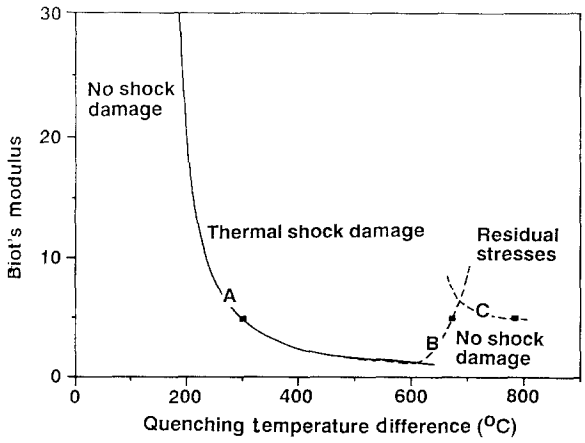

Figure 6 Thermal shock damage map of glass plate.

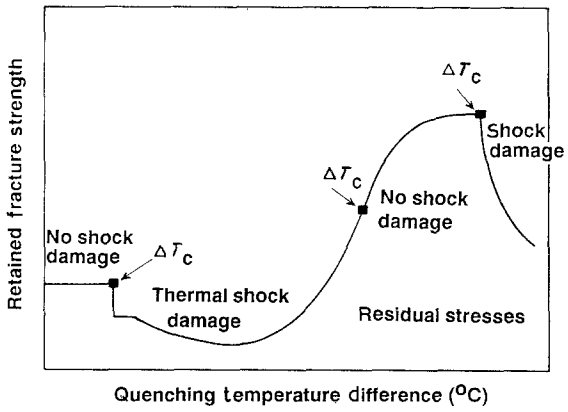

Figure 7 Thermal shock-induced strength degradation curve as derived from the thermal shock damage map for a quenched glass plate.

Thus, between 580 and 780 °C the glass plate can be tempered (strengthened) without thermal shock damage.

Fig. 8 illustrates the relation among residual surface stresses, initial quenching temperature, and Biot's modulus. For thermal quench conditions corresponding to a given Biot's modulus, the residual surface stresses reach a saturation value with further increase of the initial glass temperature. Therefore, the residual-stress-induced increase in the retained fracture strength also saturates (Fig. 8).

In this study, thermal shock damage was analysed for glass plates. Physically meaningful changes in the input parameters (Table I) for the numerical analysis only shift the curves, without changing the essential characteristics of the thermal shock damage map. For example, in a plot of Biot's modulus versus the quenching temperature difference, changing the fracture stress from the experimentally determined value of 101.4 MPa [27] downward to 60 MPa or upward to 160 MPa systematically shifts the numerical results with respect to the quenching temperature difference, but the general shape of the curve is largely maintained (Fig. 9). Variations in specimen thickness, surface heat transfer coefficient and thermal conductivity are encompassed by B, the Biot's modulus (Equation 4). Fig. 9 is quite important with respect to the

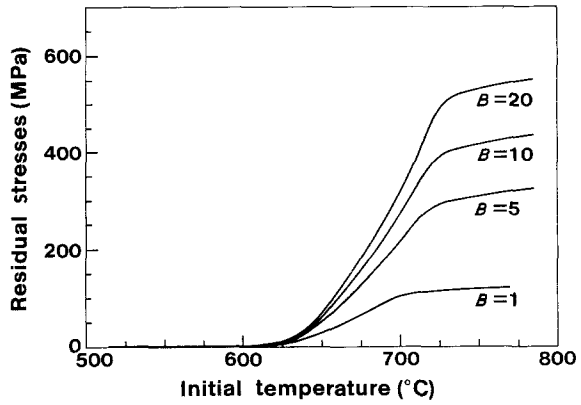

Figure 8 Relationship between residual surface stresses, initial glass temperature, and Biot's modulus B for a quenched glass plate.

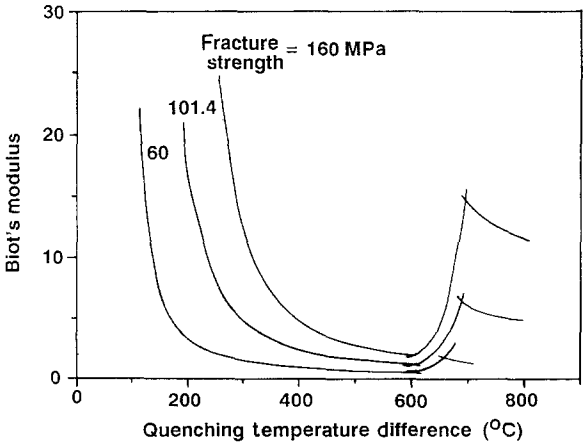

Figure 9 Shifts in the thermal shock damage map that result from assuming different flexural fracture strength values for the glass plate.

numerical modelling presented in this paper and the possibility of extending our analysis to other materials. Numerical techniques can be unstable, in that small changes in the input data may cause large swings in the results [28], but (at least with regard to changes in the fracture stress) the technique presented here seems to be stable.

Therefore, the map may apply also to those ceramic materials which are viscoelastic at high temperature. Gebauer and co-workers [9, 10] and Ohira and Bradt [11] quenched aluminosilicate rods into a silicone oil bath over a range of different quench temperature differences and obtained a strength degradation curve similar to Fig. 7. Gebauer and co-workers [9, 10] proposed that viscous flow in the glassy grain boundary phases might account for the observed strength changes. The analysis in the present study shows that the viscous flow of glass yields the same "shape" of a strength distribution curve as observed experimentally by them.

4. Concluding remarks

Thermal shock-damage studies of ceramics typically focus on thermal quenching from below the annealing temperature. In this paper, the shock damage of glass plates quenched from both above and below their annealing temperature was analysed. The heat transfer characteristics of the quench bath, the initial material temperature, and material properties determine whether quenching a glass plate produces thermal shock damage and/or produces residual stress. The analysis also indicates that thermal quench from below the glass annealing temperature leads to an increase in shock damage probability with increase of quench temperature difference, ΔT. Viscous flow occurs when a glass is quenched from above the annealing temperature. While viscous flow reduces the transient surface tensile stress, the viscous flow promotes the eventual development of residual tensile stresses in the plate's interior. Thus, damage-free tempered glass will be restricted to a certain range of ΔT.

The theoretical analysis presented here for tempered glass plates may apply also to those ceramic materials which are viscoelastic at high temperature. Although there are similarities between the behaviour predicted in this study and the experimental results in the literature for polycrystalline ceramics quenched from high temperatures, additional study is needed on the quench behaviour of ceramics containing a significant glassy grain boundary phase.

References

1. D. JOHNSON-WALLS, M. D. DRORY and A. G. EVANS, *J. Amer. Ceram. Soc.* **68** (1985) 363.
2. R. BADALIANCE, D. A. KROHN and D. P. H. HASSELMAN, *ibid.* **57** (1974) 432.
3. D. P. H. HASSELMAN, R. BADALIANCE and E. P. CHEN, in "Thermal Fatigue of Materials and Components", ASTM STP 612 (1976) pp. 55–68.
4. H. KAMIZONO, *J. Mater. Sci. Lett.* **3** (1984) 588.
5. D. P. H. HASSELMAN, *J. Amer. Ceram. Soc.* **52** (1969) 600.
6. A. F. EMERY and A. S. KOBAYASHI, *ibid.* **63** (1980) 410.
7. F. V. TOOLEY, "Handbook of Glass Manufacture", Vol. 1 (Ogden, New York, 1961) p. 391.
8. N. A. TRAVITZKY, D. G. BRANDON and E. Y. GUTMANAS, *Mater. Sci. Engng* **71** (1985) 77.
9. J. GEBAUER and D. P. H. HASSELMAN, *J. Amer. Ceram. Soc.* **54** (1971) 468.
10. J. GEBAUER, D. A. KROHN and D. P. H. HASSELMAN, *ibid.* **55** (1972) 198.
11. H. OHIRA and R. C. BRADT, *ibid.* **71** (1988) 35.
12. H. P. KIRCHNER, "Strengthening of Ceramics" (Dekker, New York, 1979) pp. 31–79.
13. B. A. BOLEY and J. H. WEINER, "Theory of Thermal Stresses" (Wiley, New York, 1960) p. 277.
14. E. H. LEE, T. G. ROGERS and T. C. WOO, *J. Amer. Ceram. Soc.* **48** (1965) 480.
15. O. S. NARAYANASWAMY and R. GARDON, *ibid.* **52** (1969) 554.
16. F. KREITH, "Principles of Heat Transfer" (International Textbook Co., Scranton, Pennsylvania, 1965) p. 174.
17. W. D. KINGERY, H. K. BOWEN and D. R. UHLMANN, "Introduction to Ceramics" (Wiley, New York, 1976) pp. 816–822.
18. R. C. BUCHANAN, "Ceramic Materials for Electronics" (Dekker, New York, 1986) p. 8.
19. L. W. MORLAND and E. H. LEE, *Trans. Soc. Rheol.* **4** (1960) 233.
20. R. MUKI and E. STERNBERG, *J. Appl. Mech.* **28** (1961) 193.
21. E. H. LEE and T. G. ROGERS, *ibid.* **30** (1963) 127.

22. O. C. ZIENKIEWICZ, M. WATSON and I. P. KING, *Int. J. Mech. Sci.* **10** (1968) 807.
23. R. L. FRUTIGER and T. C. WOO, *J. Thermal Stresses* **2** (1979) 45.
24. O. S. NARAYANASWAMY, *J. Amer. Ceram. Soc.* **61** (1978) 146.
25. R. M. CHRISTENSEN, "Theory of Viscoelasticity", 2nd Edn (Academic, New York, 1982) p. 5.
26. J. H. BATTEH, *J. Appl. Phys.* **54** (1983) 3769.
27. C.-C. CHIU and E. D. CASE, accepted for publication in *J. Mater. Sci.*
28. R. W. HAMMING, "Numerical Methods for Scientists and Engineers" (McGraw-Hill, New York, 1962) p. 175.

Received 14 November 1990
and accepted 10 April 1991